Potential evaluation of CO2 EOR and storage in oilfields of the Pearl River Mouth Basin, northern South China Sea

Potential evaluation of CO2 EOR and storage in oilfields of the Pearl River Mouth Basin, northern South China Sea

Pengchun LI[1,2], Xueyan Liu[1], Jiemin Lu[3], Di Zhou[1,6], Susan D. Hovorka[3], Gang Hu[4], Xi Liang[5,6]

[1]CAS Key Laboratory of Ocean and Marginal Sea Geology, South China Sea Institute of Oceanology, Guangzhou, China

[2]State Key Laboratory of Oil and Gas Reservoir Geology and Exploitation (Chengdu University of Technology), Chengdu, China

[3]Gulf Coast Carbon Center, Bureau of Economic Geology, The University of Texas in Austin,Austin, TX United States

[4]School of Petroleum Engineering, Guangdong University of Petrochemical Technology,Maoming, China

[5]University of Edinburgh Business School, Edinburgh, UK

[6]UK-China (Guangdong) CCUS Centre, Guangzhou, China

Abstract: The Pearl River Mouth Basin (PRMB) is the largest petroliferous sedimentary basin in the northern South China Sea. It is near the coastal economic zone of Guangdong province where a large number of CO_2 emission sources are located. Carbon dioxide enhanced oil recovery (EOR) represents an opportunity to promote offshore carbon capture, utilization and storage (CCUS) deployment because CO_2 flooding offers a method to recover additional oil while simultaneously sequestering anthropogenic CO_2. In this paper, a comprehensive multiparameter 'quick look' and potential evaluation method was proposed to screen and assess offshore CO_2 EOR potential. A screening scheme for the CO_2 EOR potential of reservoirs of the PRMB was also proposed using additional parameters, including reservoir properties and engineering design incorporating a dimensionless screen model and calculations. The results show that the suitability of reservoirs for CO_2 EOR and storage varies and could be categorized into four priority grades. Approximately 30 of the oil reservoirs from 10 oilfields were preferentially identified by applying the screening method for reservoirs with predicted higher ultimate recovery potentials. It was predicted that 3227×10^4t of additional oil could be produced from these reservoirs and that 3617×10^4t of CO_2 could be simultaneously stored. The sensitivity analysis shows that injection pressure (Pinj) would be more sensitive than production pressure (Pp) and well distance (L) on the CO_2 EOR and storage efficiency, indicating that EOR operations with higher Pinj may improve oil production. The prospective reservoirs include those candidates with suitability grades of I and II from the Lufeng (LF) and Huizhou (HZ) oilfield clusters, where 1164×10^4t of additional oil could be produced and 1464×10^4 t of CO_2 stored with CO_2 EOR.

Keywords: CO_2 EOR; carbon sequestration; capacity estimation; quick screening; offshore oil reservoirs

Introduction

Global and regional climate change caused by greenhouse gas emissions is still stimulating interest in the development of various technologies to reduce the concentrations of carbon dioxide (CO_2) in the atmosphere.[1–5] Many countries have set targets for reducing the emissions of greenhouse gases to mitigate global warming. Among these countries, and top on the list of CO_2 emission producers in the world, China aims to reduce 40%–45% of its CO_2 emissions per unit GDP by 2020, based on the 2005 level.[6] Carbon capture and storage (CCS) is widely recognized as a critical technology to meet the ambitious rate of 1.5/2°C agreed upon at the Twenty-first Conference of the Parties (COP) in Paris in 2015.[7]

Due to certain legal advantages and vast resource capacities, the offshore storage of CO_2 in geological strata has significant potential and offers an attractive alternative to onshore storage.[8] Offshore CO_2 storage has been successful in the Sleipner and Snøhvit offshore projects near Norway, and a number of other projects in the world are in the construction or planning phase.[9] Offshore CO_2 storage is the principal or only opportunity for CO_2 storage for regions without suitable onshore sites – regions such as Western Europe, Australia, the US Gulf Coast, Japan, and southeastern Asia.[10] In recent years, the application of CO_2-enhanced oil recovery (CO_2 EOR) in offshore oilfields has received significant attention due to the potentially enormous amount of recoverable oil,[11] but CO_2 EOR application offshore is still in a very early stage due to more complex conditions that require higher costs than those of onshore projects, owing to the unique parameters present offshore. Due to the higher costs and platform-space limitations for offshore activities, successful CO_2 EOR and storage applications in offshore oilfields requires more accurate site selection and evaluation methods than those for conventional onshore applications.

Guangdong is the largest provincial economy and one of the five low-carbon pilot provinces in China. The necessity for, and feasibility of, CCS in Guangdong were confirmed by a study carried out between 2010 and 2013.[12] Most CO_2 point sources in Guangdong are distributed along the coast, and source-sink matches can be made within a distance of 300 km.[13] The study also showed that the storage capacity onshore is limited, while the Pearl River Mouth Basin (PRMB) offshore has a very large effective CO_2 storage capacity.[14] Offshore storage is therefore recognized as the primary form of CO_2 storage for Guangdong;[12,15] later, the Guangdong offshore carbon capture, utilization and storage (CCUS) project (GOCCUS) started to be promoted. The long-term and large-scale development of offshore CO_2 storage for Guangdong has been suggested for 2030 and 2050.[10] The early opportunities believed to exist in offshore oilfields in the PRMB were screened qualitatively for their suitability for CCUS, and three fields were selected as candidates for the first demonstration project.[10,16] Unfortunately, these studies did not result in a quantitative potential evaluation, so more detailed studies are needed to reach a reasonable decision. In this study, an integrated oil reservoir database was established, which includes the major sandstone oil reservoirs in the PRMB offshore Guangdong. The substantial development, exploration, and reservoir property data made available in recent years were included in this database. This study proposes an assemblage of methods to calculate a list of oil recovery, storage potential and dimensionless reservoir parameters, which was used to evaluate the CO_2 EOR and storage potential to identify candidate sites for CCUS in sandstone oilfield clusters of the PRMB offshore Guangdong

province. The results can provide a ‘quick look’ to help the industry and government sectors to spend their increased investment in assessing these fields and can also provide a basis for Guangdong offshore CCUS development.

Geological setup

The Pearl River Mouth Basin (PRMB), with total area of ~ 200 000 km^2, is the largest sedimentary basin in the northern South China Sea (Fig. 1(A)). It is an extensional basin in a passive continental margin, formed by rifting in the Paleogene and subsequent subsidence in the Neogene.[17] The PRMB has experienced extensive geological surveying and hydrocarbon exploration since the 1970s. The source rocks in the PRMB are mainly Eocene lacustrine mudstones and Oligocene coal-bearing rocks, and the reservoirs developed mainly in the Neogene marine clastic and carbonate rocks and upper Oligocene alternating continental-marine beds. Three source-reservoir-seal assemblages formed: (1) the Palaeocene-Eocene self-contained continental assemblage developed sparsely in the northern PRMB; (2) the Palaeogene-Eocene-Miocene assemblage with sources in the continental Palaeogene within discrete sags, reservoirs in the marine Tertiary Zhuhai and Zhujiang formations, and seals in the upper Zhujiang formation; (3) the Zhujiang-Yuehai marine assemblage with sources in the Zhujiang formation, reservoirs in the Hanjiang formation, and seals in the upper Hanjiang and Yuehai formations.[17,18]

Structural traps in sandstone and carbonate buildups are the principal reservoir types in the PRMB. The oilfields are mainly located in the Zhu-I depression and northern Dongsha uplift as shown in Fig. 1(B). So far, more than 30 oilfields have been developed, most of them are small with proven reserves of less than 60 Mt, and only the LH11-1 field has proven reserves of 155 Mt.[19] These fields usually have strong bottom or lateral water drive energy; thus, water flooding has been proven to be unnecessary. The PRMB fields have several properties in common with those in west Texas and UKCS; these properties include low density and viscosity of the crude oil and high porosity and permeability of the reservoir,[17] favorable for miscible CO_2 EOR. Although the primary oil recovery factor is relatively high (40~62%) in these fields, similar to that in UKCS, this does not exclude the possibility of EOR in the later development period.

These fields are categorized into five clusters including the LF, HZ, XJ, PY and LH oilfield clusters, as shown in Fig. 1(B). Among these, the LF, HZ, and XJ clusters, which include a hundred oil layers, are marine sandstone oil reservoirs characterized by a high porosity and high permeability, strong bottom water drive energy and light crude oil. The PY fields are mostly gas fields with a few oil layers. The LH fields are carbonate oilfields with complex pore systems and heavy crude oils. The oil reservoirs in the LF, HZ, and XJ oilfield clusters were therefore evaluated in this study. These fields are located near onshore CO_2 emission sources along the coast (Fig. 1). These oilfield clusters were planned source-sink matches with onshore source clusters for the GOCCUS in 2030 and 2050.[10] The results of a buffering analysis among the sources and sites based on a GIS method show that the matching distances between onshore CO_2 emission sources and offshore oilfields are mainly 150~250 km, as shown in Fig. 2. At

this distance, the frequency percentage of CO_2 emission points is up to 65% (Fig. 2a), and the total mass of CO_2 emissions is greater than 1000 Mt (Fig. 2b). Thus, more than 70 oil reservoirs in the LF, HZ, and XJ oilfield clusters were selected for study, and their CO_2 EOR potential was quickly screened and assessed in this paper.

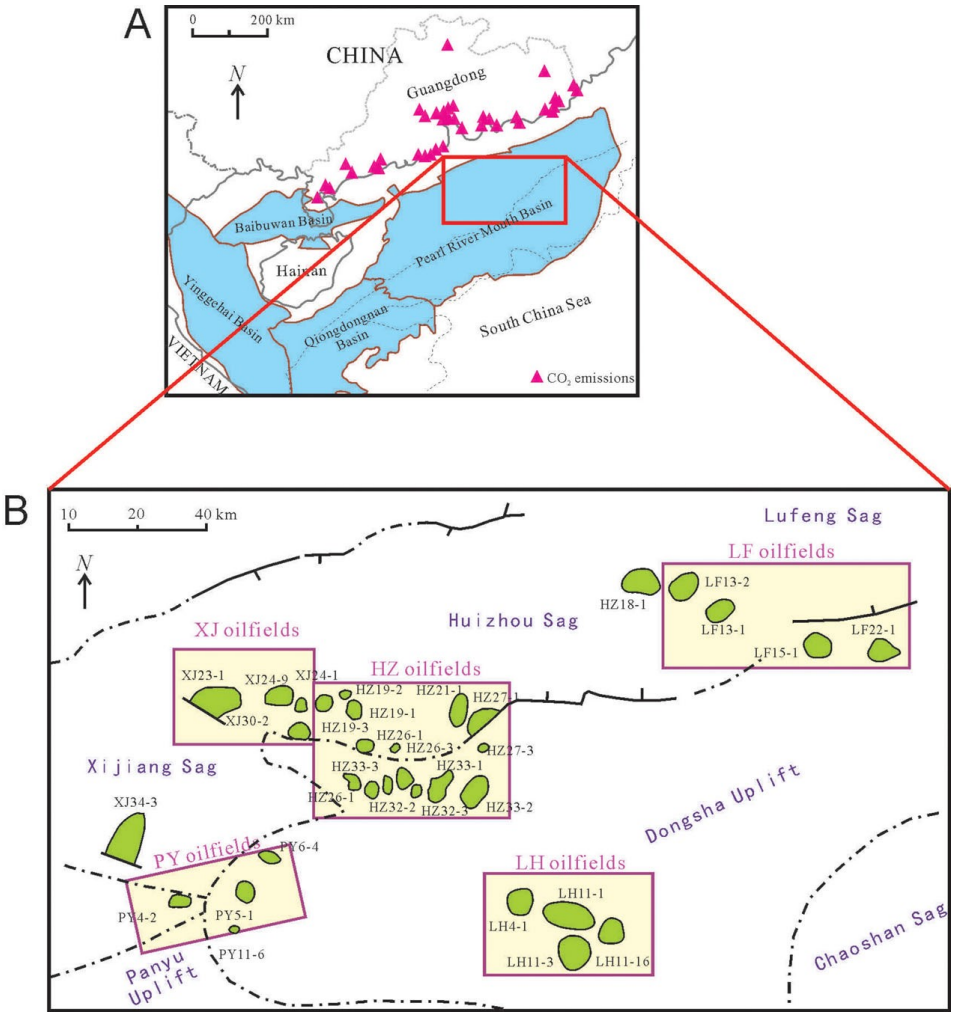

Figure 1. Maps showing structure subdivision and oilfield location (A and B, respectively), offshore Guangdong province, southern China, together with CO_2 emission sources in A (CO_2 emission sources from Huang;[20] oilfields from Luo[21]).

Methodology

The main focus of an evaluation of CO_2-EOR potential in a carbon-constrained environment is to estimate the oil-recovery efficiency and the volume of sequestered CO_2 for various operating scenarios.[22] Most EOR screening methods are geared towards optimizing CO_2 EOR reservoir performance (incremental oil production), ignoring CO_2 sequestration in petroleum industry operations. Although a reservoir simulation can be used for a relatively precise capacity assessment if detailed reservoirs data are available, quick methods are mostly used to calculate capacity for preliminary site-screening purposes. The oil recovery potential of each reservoir is assumed to be close to its ultimate primary and secondary recovery;[23] thus, the quick prediction of CO_2 flooding performance for large number of oil pools is expressed in relation to the target original oil in place (OOIP).[22,24] Furthermore, quantitative screening models

including CO_2 Prophet, the CO_2 Predictive Model, Kinder Morgan's scoping models and models by Rivas et al.[25] and Diaz et al.[26] have been developed. Although these methods are based on theoretical calculations, numerical simulations and field experience can be applied relatively easily; however, these methods also need more detailed reservoir information, are too time consuming, or did not produce quantitative data for oil recovery and CO_2 storage.[27] Thus, these methods are not suitable for the batch analysis of a large number of oil layers.

The scaling method outputs a result extrapolated from one scale to another scale.[28] Wood[29] developed dimensionless groups for continuous gravity-stable CO_2 flooding of homogeneous reservoirs with high vertical permeability and large dip angles to scale miscible CO_2 flooding and storage. This multiparameter method was developed not only to facilitate inputting more reservoir properties but also to calculate the result quickly using an Excel spreadsheet. It is ideal for quickly screening large databases of reservoirs for the most attractive CO_2 EOR and storage candidates, but to apply this method, the potential of CO_2 EOR and storage must first be evaluated quantitatively to determine the oil recovery and CO_2 storage capacities.

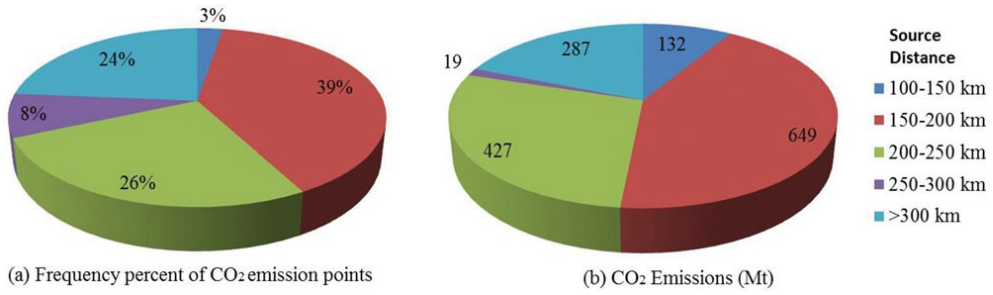

Figure 2. Pie charts of source and site matching relationship, showing frequency percentage of CO_2 emission points (a) and total mass of CO_2 emissions, (b) for different distances to offshore oilfield sites.

On the other hand, the evaluation method for CO_2 storage capacity has focused on two main areas: (1) the assessments of total capacities per scale including country, basin, region, local and site-specific scales, and (2) the risk assessment and uncertainty analysis of CO_2 storage.[30] The first approach has resulted in inventories and global atlases, with an emphasis on theoretical and effective storage capacities based on material balance, analogy methods, and different trapping mechanisms.[31–35] Such capacities are being used by modelers and policy makers to set the physical boundaries for national deployment of CCUS. The second approach has resulted in a screening and ranking framework (SRF) for site risk assessments on the basis of health, safety, and environment (HSE) issues arising from CO_2 leakage.[36–39] Almost all of these frameworks are based on quantitative mathematical modeling and only a few semiquantitative assessments have been developed;[30] more time and effort should be given to this work, especially for the early stage offshore CCUS project in China.

This paper mainly focuses on the screening potential of an oil reservoir for CO_2 storage associated with EOR. Thus, based on previous research, a modified evaluation process was proposed combining a multiparameter screening model and a mass balance calculation approach. Moreover, the reservoir and injection operation properties were used for calculating

and could yield more reliable results because this is more physically reasonable than using the volumetric equations directly.

Multiparameter screening model

Wood[29] derived seven important dimensionless groups of parameters, the effective aspect ratio (R_L), the CO_2-oil mobility ratio (M_g^o), the buoyancy number (N_g^o), the injection pressure (P_{injD}), the production pressure (P_{prod}), the initial oil saturation (S_{oi}) and the residual oil saturation to water (S_{orw}), to scale continuous CO_2 flooding in a Gulf Coast reservoir. The model works by inputting the dimensionless groups into a simulator to produce output parameters.[23,27,29] The five output parameters were modeled with the normalized dimensionless group values using response surface fitting as the results of the output from the simulator. The first parameter is the dimensionless oil breakthrough time (t_D) at which significant amounts of oil are recovered. Recovery at all points before this time is assumed to be zero. The three oil recoveries are the first dimensionless recovery (R_{D1}), second dimensionless recovery (R_{D2}), and third dimensionless recovery (R_{D3}) at t_D = 0.8, 1.0, and 1.2, respectively. Dimensionless recovery is the fraction of the total pore volume recovered, and not the typical measure of the percentage of the original oil in place (% OOIP) recovered. Only one parameter is used to model CO_2 storage: the pore volumes of CO_2 storage, S_{CO2}, at the final dimensionless time, t_D = 1.2. The dimensionless breakthrough time, recovery, and CO_2 storage can therefore be used to make an accurate estimation and ranking of its oil recovery and CO_2 storage potential. TheWood's[29] multiparameter model uses dimensionless groups that are necessary to successfully scale continuous CO_2 flooding for a typical line-drive pattern, which is most applicable to oil reservoirs in the PRMB of this study. Therefore, in this paper, the dimensionless model was used to scale CO_2 flooding and evaluate the oil recovery and CO_2 storage potential of oilfields in the PRMB.

Capacity estimations

The methods for calculating CO_2 storage and EOR potentials of oil reservoirs depend on the reservoir status, CO_2 injection process, and CO_2 storage mechanism. In the PRMB, there are only primary recovery oil reservoirs because of the strong water drive. There are therefore several types of capacities to determine for the CO_2 EOR process, including the theoretical and effective storage capacities (the volume of CO_2 that can potentially be stored) and the amount of crude oil that can be produced during CO_2 EOR operations. The following sections will discuss the calculations of the EOR and CO_2 storage capacities for the reservoir.

Calculation of effective CO_2 storage capacity in oil reservoir

A quick assessment of the theoretical and effective CO_2 storage capacity in an oil reservoir is a very important factor for CO_2 EOR and storage site selection. In the study area, the oilfields are usually developed by natural depletion because of the strong water drive. Although formation water would invade the reservoir as the pressure declines because of production, leading to a decrease in the pore space available for CO_2 storage, CO_2 injection can partially

reverse the aquifer influx, thus making more pore space available for CO_2.[40] In this study, for the quick-look assessment objective, it is assumed that the pore volume represented by the oil production is available in the reservoir for CO_2 storage. The theoretical storage capacity of CO_2 in an oil reservoir was therefore defined as the volumetric-based CO_2 storage estimation using the original oil in place (OOIP) value calculated by the standard industry methods provided by the Carbon Sequestration Leadership Forum (CSLF).[34] The effective storage capacity for the CO_2 storage in the oil reservoirs under in situ conditions, M_{CO2e}, is given by:

$$M_{CO2e} = \rho_{CO2r} \times R_f \times OOIP/B_f \times C_e \quad (1)$$

where ρ_{CO2r} = CO_2 density under reservoir conditions; OOIP = original oil in place; R_f = oil recovery factor; B_f = the formation volume factor that converts the oil volume from standard conditions to the *in situ* conditions; and C_e = CO_2 storage efficiency factor.

The CO_2 storage efficiency factor is likely variable, depending on the reservoir characteristics; this variability explains the wide range of incremental oil recovery and CO_2 utilization.[31] Unfortunately, few studies have estimated C_e values. According to Bachu and Shaw,[32] C_e = $C_{eff} \times C_{aq}$, where $C_{eff} < 1$ is the effective storage coefficient and C_{aq} is the relative reduction in storage capacity caused by the effects of formation water influx. The coefficient C_{eff} represents the CO_2 mobility and density with respect to the oil and water, water saturation, and reservoir heterogeneity. For an oil reservoir, a value of C_{eff} = 0.5 was considered reasonable, and C_{aq} = 81% to 25% with an average 50%.[41] The oil recovery factors in the PRMB sandstone oil reservoirs studied in this paper are primarily high and strongly water driven;[17] therefore, the mean C_e value normally used for the reservoirs of this study is $C_e = 0.5 \times 0.5 = 0.25$.

Calculation of additional oil production from CO_2 EOR

The additional oil production of reserves due to CO_2 EOR is determined by applying an extra recovery factor, and the extra recovery factor from the CO_2 EOR operation is taken as a percentage of the OOIP. In this study, therefore, the additional oil produced due to CO_2 EOR is calculated using the approach from Stevens[42] and Hendriks et al.[24] as follows:

$$N_p = OOIP\ R_{CO2}C \quad (2)$$

where N_p = extra oil production due to CO_2 EOR; R_{CO2} = recovery factor increment because of CO_2 EOR; and C = contact coefficient of CO_2 and crude oil, which is generally 0.75.[42]

To calculate the R_{CO2} due to CO_2 injection, an empirical relationship between the oil gravity (API) and recovery increment was proposed based on seven Permian Basin (US) EOR projects.[42] More CO_2 will be required to produce one barrel of low-API oil than that required to produce a barrel of high-API oil. A low value of 5%, a best estimate of 12%, and a high estimate of 20% were therefore proposed for the EOR calculation. The API gravity of oil in oilfields of this study is of 42~46%,[17] which indicated that a high R_{CO2} (12%~20%) should be assigned to the oilfields in this study. Combined with the offshore experience value of reservoir recovery, which is assumed to be 15% of the OOIP based on the EOR history in the Gulf Coast,[23] the R_{CO2} value of 15% was reasonably assumed in this study.

Calculation of CO_2 storage capacity from CO_2 EOR

The estimation of CO_2 storage capacity in CO_2 EOR projects could not be based on the reservoir volume for storage at reservoir conditions; however, detailed case-by-case numerical reservoir simulations could predict the reservoir behavior, the amount of additional recoverable oil, and the amount of CO_2 that needed to be injected.[31] Many countries, especially the US and EU, and organizations have conducted many CO_2 EOR projects and obtained valuable observations. For this quick estimation method, the CO_2 utilization coefficient is used to calculate the total CO_2 storage capacity due to CO_2 EOR as Shen et al.[43] proposed:

$$M_{CO2R} = N_p C_{CO2} \tag{3}$$

where M_{CO2R} = volume of CO_2 that can be potentially sequestered, t; N_p = cumulative oil production due to CO_2 injection, m^3; and C_{CO2} = CO_2 utilization coefficient, i.e., the ratio of net CO_2 injection versus produced oil, t/m^3. In this study, no distinction was made between miscible and immiscible flooding. Based on observations reported in the literature,[24,43] the value of C_{CO2} varies for reservoirs and ranges from 0.9-5.0 t/m^3; a minimum estimate of 1.0 t/m^3, a moderate estimate of 3.0 t/m^3, and a maximum estimate of 5.0 t/m^3 were proposed in this study.

Parameters

Data sources

The data for this study were generated by gathering engineering information from several sources, including the Atlas of Oil and Gas Basins, China Sea,[18] Development of Oil and Gas Fields of China, Volume of Oil and Gas Fields in Eastern South China Sea,[17] and engineering research books edited by Luo et al.[44] and Luo.[21] The geological, petroleum, and production data to 2005 or 2010 are from data published in Zhu and Mi[18] and CNOOC.[45] We mainly used the data from these publications as a basis for our study, and the production history data was partially updated to the end of 2010.

Parameters were collected from the 12 oilfields, from the LF, HZ, and XJ oilfield clusters, which include 72 oil reservoirs, to build the database for the screening calculation and analysis. The database includes petro-physical data, fluid characteristics, and geological information, along with production information and location data. The screening model at a reservoir scale requires 10 parameters, including reservoir thickness, temperature, pressure, oil density, and injection pressure for all oil layers. The parameters in the database were listed in Table 1.

General parameter values

The viscosities of water, oil, and CO_2 in units of cP and the densities of the oil and CO_2 in units of kg/m^3 were calculated using the equations as shown inWood[29] and Wood et al.[27] In this paper, in general, the assigned vertical permeability is $k_z = 0.1k_x$ (horizontal permeability, k_x),

injection pressure is P_{inj} = 0.75×1.5P_{inF} (initial formation pressure, P_{inF}), and production pressure is P_{pro} = 0.5 P_{inF}.

The input parameters of the oilfields needed in the dimensionless model mainly include rock and fluid variables and engineering variables, as shown in Table 1. We set reservoir dip (α) as a constant value of 0° due to the sensitivity within a relatively small range (less than 3°) in these reservoirs. Additionally, the endpoint relative permeability of the oil (k_{ro}^{o}) and endpoint relative permeability of the gas (k_{rg}^{o}) are given as two experiential values, and the distance between injector and producer (L) is given based on the field condition. The reservoir thickness (H), permeability in the x direction (k_x), reservoir temperature (T), average reservoir pressure (P), oil density (ρ_{oil}), and oil viscosity (μ_{oil}) are obtained or interpolated from Liu;[17] the CO2 density (ρ_{CO2r}) and CO_2 viscosity (μ_{CO2}) are calculated based onWood.[29] The initial oil saturation (S_{oi}), which means the oil saturation at the start of CO_2 injection, is calculated as follows:

$$S_{oi} = S_{oo} \times PV_o + S_{oa} \times PV_a \tag{4}$$

where S_{oo} presents residual oil saturation in the reservoir, and S_{oa} means the residual oil saturation in the reservoir and is given as 20%. Additionally, the ratio of pore volume in the oil layer and water layer over the sum of those two are PV_o and PV_a, respectively.

Minimum miscibility pressure determination

Minimum miscibility pressure (P_{MM}) is of utmost importance for CO_2 flooding and could significantly influence the flooding mechanism and recovery effectiveness. An estimate of the minimum miscibility pressure (P_{MM}) was necessary to calculate the injection and producing pressure groups. Several correlations exist in the literature, including those described by Jarrell et al.[46] and Holm and Josendal[47] and extended by Mungan[48] and others. However, because of the limitation of no test data of the oil component, the P_{MM} cannot be estimated from the molecular weight (MW) of the C_{5+} components of the reservoir crude oil. In this paper, the empirical correlation proposed by Mungan[49] and He et al.[50] was used to calculate P_{MM} quickly by using the following form:

$$P_{MM} = -329.558 + (7.727 \times MW \times 1.005^{T}) - (4.377 \times MW) \tag{5}$$

where T is the reservoir temperature;MW= $(7864.9/G)^{1/1.0386}$, which is the molecular weight of the C_{5+} components, and G is the oil API gravity.

Table 1. Reservoir property parameters used in quick screening model and estimation.

No.	OOIP ($\times 10^4$ m^3)	T (°F)	P (psi)	H(ft)	Kx (mD)	Kz (mD)	μ_{oil}	μ_{CO_2}	ρ_{oilsur} (kg/m^3)	ρ_{oilres} (kg/m^3)	$\rho_{CO_2 res}$ (kg/m^3)	P_{inj} (psi)	P_p (psi)	Soi (%)	Soiav	R_f	MMP (psi)
1	164	257	3879.8	19.4	271.3	27.13	0.32	0.054	798	634	524.5	4661.7	(psi)	61.0	22.6	0.599	3191.7
2	368	262.4	3943.6	42.7	317.3	31.73	0.41	0.059	800	655	523.5	4733.5	2103.8	63.4	27.1	0.456	3341.0
3	191	263.48	4024.8	12.5	282.3	28.23	0.41	0.064	800	655	534.3	4805.3	2135.7	61.1	25.2	0.511	3364.4
4	245	267.8	4033.5	27.2	192.3	19.23	0.36	0.066	802	642	527.6	4766.1	2118.3	61.6	21.2	0.645	3199.1
5	232	267.584	4064.0	69.9	68	6.8	0.35	0.068	802	647	533.0	4836.3	2149.5	55.3	27.5	0.188	3211.1
6	637	269.6	4091.5	131.9	205.3	20.53	0.32	0.070	804	747	533.9	4867.3	2163.2	59.3	25.2	0.236	3355.7
7	—	275	4091.5	68.9	130.4	13.04	0.32	0.072	804	747	524.2	4867.3	2163.2	48.4	24.2	0.023	3473.7
8	317	144.428	2328.2	9.8	1000	100	17.10	0.047	903	879	615.7	2752.6	1223.4	56.7	37.0	0.287	2304.6
9	2873	158	2520.1	23.0	1000	100	7.00	0.046	903	879	594.8	3077.3	1367.7	63.5	28.9	0.521	2559.3
10	1114	180.932	3130.8	15.0	1000	100	6.00	0.048	903	879	613.6	3720.2	1653.4	60.9	32.8	0.426	3030.8
11	979	194	3332.0	9.4	1000	100	5.00	0.047	871	879	602.5	4046.6	1798.5	67.1	23.4	0.641	2951.4
12	1026	210.2	3672.5	16.4	1000	100	4.00	0.049	876	879	602.3	4372.9	1943.5	57.8	26.6	0.519	3303.2
13	254	235.04	3334.4	90.6	2019	201.9	3.88	0.038	872	821	493.7	3787.1	1683.2	63.8	22.8	0.524	2926.8
14	633	242.42	3549.1	40.7	1300	130	3.38	0.041	875	817	508.6	4028.6	1790.5	38.6	20.5	0.459	3010.2
15	1041	242.42	3587.1	135.2	1300	130	3.87	0.043	871	822	514.5	4071.4	1809.5	54.6	22.8	0.459	3049.8
16	—	239.72	3641.9	82.7	1323	132.3	3.80	0.044	829	823	529.2	4162.4	1850.0	64.4	31.3	0.439	2279.3
17	1908	194	2298.8	131.2	2424	242.4	4.75	0.034	856	800	394.1	2667.8	1185.7	64.4	28.3	0.300	2160.0
18	505	206.6	2467.5	49.2	637	63.7	4.60	0.034	857	824	397.7	3007.2	1336.5	60.6	21.2	0.617	1967.1
19	—	206.6	2783.6	38.4	660	66	4.60	0.036	823	824	472.7	3168.7	1408.3	46.5	25.5	0.080	1967.1
20	128	206.6	2732.5	47.2	569	56.9	4.60	0.036	870	824	461.7	3237.2	1438.8	53.2	23.2	0.368	2447.0
21	—	224.6	2876.1	25.9	1372	137.2	4.60	0.034	860	824	440.4	3279.7	1457.6	53.6	25.0	0.096	2237.5
22	809	224.6	2928.3	37.4	1088	108.8	3.15	0.034	860	794	450.9	3669.6	1630.9	75.8	23.8	0.514	2357.7
23	177	228.2	3285.1	78.7	1323	132.3	1.98	0.038	834	770	503.1	3717.0	1652.0	59.6	25.5	0.047	2135.8
24	236	228.2	3265.6	32.8	1096	109.6	2.02	0.038	834	780	500.1	3777.3	1678.8	68.0	24.2	0.529	2247.7
25	380	230	3251.7	17.6	235	23.5	2.02	0.037	822	780	493.4	3821.4	1698.4	71.9	32.0	0.377	2323.5
26	1663	230	3333.9	176.0	1047	104.7	1.67	0.038	827	773	506.0	3870.3	1720.1	69.6	23.6	0.489	2196.1
27	436	233.6	3354.1	93.2	809	80.9	1.93	0.038	853	804	500.2	3958.4	1759.3	64.9	24.9	0.270	2645.1

(continued)

Table 1. Continued

No.	OOIP ($\times 10^4$ m^3)	T (°F)	P (psi)	H(ft)	Kx (mD)	Kz (mD)	μ_{oil}	μ_{CO_2}	ρ_{oilsur} (kg/m^3)	ρ_{oilres} (kg/m^3)	ρ_{CO_2}res (kg/m^3)	P_{inj} (psi)	P_p (psi)	Soi (%)	Soiav	R_f	MMP (psi)
28	63	181.4	2284.3	26.2	846	84.6	1.50	0.035	819	752	437.2	2715.1	1206.7	51.9	23.7	0.312	1280.7
29	83	188.6	2442.4	26.2	963	96.3	1.50	0.036	822	752	452.8	2863.6	1272.7	59.2	28.8	0.250	1357.0
30	753	197.6	2419.2	32.8	742	74.2	1.50	0.035	825	752	414.6	3031.7	1347.4	72.2	22.7	0.669	1755.0
31	39	197.6	2419.2	9.8	308	30.8	1.50	0.035	825	752	414.6	3031.7	1347.4	43.1	16.8	0.669	1755.0
32	251	219.2	2628.7	32.8	83	8.3	1.50	0.034	822	752	400.1	3031.7	1347.4	54.8	31.2	0.160	1714.1
33	49	219.92	3166.2	16.4	244.3	24.43	2.61	0.038	859	806	505.8	3692.5	1641.1	55.0	27.8	0.297	2555.2
34	14	222.8	3111.1	16.4	244.3	24.43	2.61	0.036	859	806	489.0	3692.5	1641.1	40.9	21.9	0.422	2606.7
35	183	225.32	3232.9	24.0	341.1	34.11	2.61	0.038	892	806	502.3	3767.5	1674.5	59.1	35.6	0.284	2756.7
36	286	230	3241.6	36.4	623.1	62.31	2.61	0.037	852	806	491.8	3940.5	1751.3	75.7	23.3	0.643	2738.6
37	334	230	3402.6	55.4	710.4	71.04	2.61	0.040	865	806	516.2	3974.8	1766.6	56.4	29.4	0.328	2738.6
38	401	234.5	3525.9	75.5	512.1	51.21	2.61	0.042	844	806	523.5	4151.0	1844.9	71.8	29.1	0.405	2434.3
39	2902	206.6	2767.3	61.0	2729	272.9	2.30	0.036	823	788	469.2	3235.6	1438.0	74.5	23.4	0.627	2085.8
40	130	222.98	3111.8	14.4	247	24.7	2.30	0.036	854	788	488.7	3594.6	1597.6	38.2	30.5	0.202	2016.9
41	98	224.6	3190.8	8.2	705	70.5	2.30	0.037	902	788	497.5	3752.9	1667.9	59.1	37.4	0.367	2683.1
42	14	224.6	3190.8	3.9	405	40.5	2.30	0.037	902	788	497.5	3752.9	1667.9	43.3	27.4	0.367	2683.1
43	195	224.6	3190.8	21.0	1438	143.8	2.30	0.037	902	788	497.5	3752.9	1667.9	57.9	34.3	0.339	2683.1
44	192	226.4	3354.7	48.6	815	81.5	2.30	0.039	807	788	518.2	3937.2	1749.9	43.7	23.8	0.345	2066.5
45	642	168.8	2610.1	26.2	827	82.7	12.40	0.044	890	869	568.6	3074.1	1366.3	60.0	41.6	0.529	2441.5
46	350	192.2	2818.2	12.5	887	88.7	5.80	0.040	865	817	525.4	3304.1	1468.5	64.6	45.3	0.529	2119.6
47	48	192.2	2850.4	5.9	342	34.2	5.80	0.040	870	817	531.6	3344.9	1486.6	53.3	36.9	0.529	2119.6
48	740	183.2	2907.2	49.2	1982	198.2	6.40	0.044	870	855	571.4	3410.2	1515.6	76.2	39.9	0.529	2484.3
49	16	183.2	2995.5	6.6	1328	132.8	6.40	0.045	870	855	586.0	3508.1	1559.2	64.9	44.9	0.529	2484.3
50	22	183.2	3105.7	4.9	1048	104.8	6.40	0.047	870	855	602.8	3632.1	1614.3	58.6	40.6	0.529	2484.3
51	10	183.2	3140.5	3.3	54	5.4	6.40	0.047	870	855	607.9	3671.3	1631.7	52.5	36.3	0.529	2484.3
52	216	201.2	3282.6	7.5	365	36.5	2.70	0.044	827	796	575.1	3818.1	1696.9	66.3	47.8	0.529	2016.2
53	491	201.2	3288.2	7.9	802	80.2	2.70	0.044	827	796	575.9	3858.9	1715.1	68.5	44.1	0.529	2016.2
54	234	201.2	3413.0	6.9	828	82.8	2.70	0.046	827	796	593.1	3858.9	1715.1	63.7	61.0	0.529	2016.2

(continued)

Table 1. Continued

No.	OOIP ($\times 10^4$ m^3)	T (°F)	P (psi)	H(ft)	Kx (mD)	Kz (mD)	μ_{oil}	μ_{CO_2}	ρ_{oilsur} (kg/m^3)	ρ_{oilres} (kg/m^3)	ρ_{CO_2}res (kg/m^3)	P_{inj} (psi)	P_p (psi)	Soi (%)	Soiav	R_f	MMP (psi)
55	760	199.4	3310.6	32.8	1510	151	2.30	0.045	833	799	584.1	3862.2	1716.5	70.5	44.8	0.529	2022.5
56	—	199.4	3212.5	5.0	96	9.6	2.30	0.043	821	799	570.0	3893.2	1730.3	47.6	18.0	0.622	1926.4
57	—	201.2	3227.0	8.7	684	68.4	2.30	0.043	821	799	566.9	3909.5	1737.6	66.3	25.1	0.622	1952.2
58	—	203	3232.8	5.5	244	24.4	2.30	0.043	821	799	562.7	3916.0	1740.5	45.6	17.2	0.622	1978.1
59	—	203.72	3264.7	26.2	764	76.4	2.30	0.043	821	799	565.4	3951.9	1756.4	72.8	24.0	0.622	1988.6
60	—	206.6	3331.4	6.2	245	24.5	2.30	0.043	821	799	567.0	4027.0	1789.8	51.0	19.3	0.622	2030.8
61	—	212	3364.8	16.4	528	52.8	2.16	0.043	821	772	557.1	4064.5	1806.4	54.0	20.2	0.622	1921.7
62	41	212	3364.8	11.8	439	43.9	2.16	0.043	821	772	557.1	4064.5	1806.4	66.4	25.1	0.622	1921.7
63	16	212	3377.8	7.2	284	28.4	2.16	0.043	821	772	558.9	4079.2	1813.0	57.0	21.5	0.622	1921.7
64	—	212	3377.8	5.0	114	11.4	2.16	0.043	821	772	558.9	4079.2	1813.0	46.3	17.5	0.622	1921.7
65	3	212.36	3435.8	6.2	112	11.2	2.16	0.044	821	772	566.1	4144.5	1842.0	53.8	20.3	0.622	2117.0
66	16	212.9	3450.3	11.5	217	21.7	2.16	0.044	821	772	566.6	4160.8	1849.2	55.3	20.9	0.622	2125.2
67	58	212	3537.4	11.3	340	34	2.52	0.046	837	801	580.6	4258.7	1892.7	64.2	24.3	0.622	2111.5
68	3	210.02	3560.6	14.4	118	11.8	2.52	0.047	837	801	588.7	4284.8	1904.3	58.3	22.0	0.622	2208.0
69	—	215.6	3621.5	3.9	52	5.2	2.52	0.047	819	801	582.5	4353.3	1934.8	61.7	23.3	0.622	2166.6
70	33	217.4	3643.2	29.2	413	41.3	1.63	0.047	819	777	581.0	4377.8	1945.7	62.9	23.8	0.622	2050.4
71	99	217.4	3678.9	14.8	209	20.9	1.63	0.048	856	777	585.3	4417.9	1963.5	59.3	22.4	0.622	2194.5
72	—	215.6	3737.5	49.2	570	57	3.02	0.050	827	819	596.9	4483.8	1992.8	67.2	22.8	0.622	2534.9

Note: All these values are referenced from Liu,[17] Zhu[18] and Luo.[21] According to the reservoir properties and engineering observations, the other values including L, α, K_{ro}, K_{rg} *and* S_{orw} were set to constant values of 900, 0, 0.6, 0.3 and 20, respectively. The minimum miscible pressure (MMP) is calculated using Eqn (5), as stated in the text. — denotes no value collected.

Results

Dimensionless screening

Screening results

As mentioned above, five outputs were used to model oil recovery potential and CO_2 storage. These results are shown in Table 2. The first critical parameter is the dimensionless oil breakthrough time (t_D^0), at which a significant amount of oil is recovered. For the model equation described, the most important fluid property groups in modeling t_D^0 were S_{oi} and S_{orw}, which are important in determining whether or not mobile oil is present at the beginning of the CO_2 flood. If mobile oil is present, oil will be produced almost immediately and therefore the t_D^0 will be close to 0; however, if only residual oil is present, oil will be produced much later in the flood and t_D^0 will be higher. The value of tD° changes within the large range of 0.1 PV to 1.1 PV. According to the statistical analysis results shown in Fig. 3, the frequency percentage of $t_D^0 < 0.4$ PV is only 10%, the percentage for 0.4–0.6 PV is 18%, the percentage for 0.6–0.8 PV is 43%, and the percentage of $t_D^0 > 0.8$ PV is 29%.Most oil reservoirs, 72%, therefore have less mobile oil, and more residual oil is present in reservoirs with higher t_D^0 values of more than 0.6 PV; only 28% of the reservoirs have more mobile oil, as suggested by lower t_D^0 values of less than 0.6 PV, as shown in Fig. 3. The analysis of the average oilfield shows that the t_D^0 value of the XJ24-1 oilfield is largest at 0.93 PV, and that of the XJ24-3 oilfield is smallest at 0.38 PV; the other oilfields have t_D^0 values between 0.5 and 0.8 PV, and eight fields are almost greater than 0.6 PV, as shown in Fig. 4.

Three dimensionless recoveries were used to describe the increasing recovery potential: the dimensionless recoveries at $t_D = 0.8(R_{D1})$, $t_D = 1.0$ (R_{D2}) and $t_D = 1.2(R_{D3})$. The dimensionless recovery at any given time is the percentage of the oil in place at the beginning of the CO_2 flood. As the dimensionless recovery model describes,[29] the Soi is the most important group for R_D, which plays a large role in the presence or absence of mobile oil at the start of the CO_2 flood. Mobile oil is easier to recover than residual oil; floods have greater S_{oi} values at the start of CO_2 flooding, and thus larger amounts of mobile oil will produce larger dimensionless recoveries. The statistical analysis results indicate that the R_{D1} values of 59 reservoirs (accounting for 82%) are less than 30%, and 13 reservoirs (18%) have R_{D1} values greater than 30%, as shown in Fig. 5(a–b). Only three reservoirs have R_{D1} values greater than 40%. The maximum R_{D1} is 47.75%. The R_{D2} values of 20 reservoirs (accounting for 28%) are less than 10%, and most reservoirs, 47 reservoirs, have R_{D2} values that vary from 10% to 50%, whereas only five reservoirs (7%) have R_{D2} values greater than 50%, as shown in Fig. 5(c–d). The maximum R_{D2} is 66%. The R_{D3} values of 17 reservoirs (accounting for 24%) are less than 10%, and 50 reservoirs (69%) have R_{D3} values that vary from 10% to 60%, whereas only five reservoirs have R_{D3} values greater than 60%, as shown in Fig. 5(e–f). The maximum R_{D3} is 73%, accounting for only 7% of the reservoirs.

The average values of the statistical analysis results at the oilfield scale are listed in Table 3 and shown in Fig. 6. The average R_{D1} varies from 7.7% to 43.1%, and the maximum is 16.5

No.	t_D^0 (PV)	R_{D1} (%)	R_{D2} (%)	R_{D3} (%)	S_{CO_2} (PV)	Np ($\times 10^4$ t)	M_{CO_2t} ($\times 10^4$ t)	M_{CO_2e} ($\times 10^4$ t)	Min. stor. ($\times 10^4$ t)	Mid. stor. ($\times 10^4$ t)	Max. stor. ($\times 10^4$ t)
1	0.70	12.82	21.07	24.09	0.80	14.7	101.4	20.3	18.5	55.4	92.3
2	0.61	30.06	42.95	45.99	0.78	33.1	178.3	35.7	41.4	124.2	207.0
3	0.65	4.20	8.89	11.28	0.79	17.2	103.0	20.6	21.5	64.5	107.4
4	0.74	17.26	27.41	30.85	0.81	22.1	160.5	32.1	27.6	82.7	137.8
5	0.64	36.13	51.27	54.89	0.81	20.9	64.8	13.0	26.1	78.3	130.5
6	0.66	33.95	48.94	52.49	0.80	57.6	176.6	35.3	71.7	215.0	358.3
7	0.65	29.28	42.54	45.68	0.78						
8	0.40	0.00	0.00	0.00	0.71	32.2	109.5	21.9	35.7	107.0	178.3
9	0.51	0.00	0.00	3.51	0.71	291.9	1472.4	294.5	323.2	969.6	1616.1
10	0.47	0.00	0.00	0.00	0.72	113.2	505.6	101.1	125.3	376.0	626.6
11	0.66	0.00	0.00	0.00	0.77	95.9	577.9	115.6	110.1	330.4	550.7
12	0.59	0.00	2.77	7.12	0.75	101.1	515.0	103.0	115.4	346.3	577.1
13	0.64	5.77	17.02	22.82	0.74	24.9	112.2	22.4	28.6	85.7	142.9
14	0.69	2.72	12.03	17.19	0.76	62.3	262.5	52.5	71.2	213.6	356.1
15	0.65	10.03	22.34	28.10	0.76	102.0	432.0	86.4	117.1	351.3	585.6
16	0.67	30.42	48.91	56.92	0.91						
17	0.53	4.45	16.71	23.47	0.72	183.7	452.6	90.5	214.7	644.0	1073.3
18	0.75	0.00	8.59	16.65	0.82	48.7	200.3	40.1	56.8	170.4	284.1
19	0.71	4.82	17.53	25.53	0.85	0.0					
20	0.64	0.00	8.08	14.60	0.75	12.5	40.4	8.1	14.4	43.2	72.0
21	0.66	0.00	4.37	11.61	0.80						
22	0.72	8.47	20.51	27.13	0.83	78.3	327.9	65.6	91.0	273.0	455.1
23	0.75	21.20	37.54	45.15	0.89	16.6	23.8	4.8	19.9	59.7	99.6
24	0.75	17.73	30.99	37.04	0.87	22.1	107.1	21.4	26.6	79.7	132.8
25	0.60	16.98	27.94	33.20	0.86	35.1	130.2	26.0	42.8	128.3	213.8
26	0.80	28.41	45.92	52.75	0.89	154.7	719.1	143.8	187.1	561.3	935.4
27	0.68	23.38	37.82	43.08	0.81	41.8	121.5	24.3	49.1	147.2	245.3
28	0.92	23.25	39.76	47.98	0.99	5.8	17.3	3.5	7.1	21.3	35.4
29	0.81	30.76	48.43	56.39	0.99	7.7	20.5	4.1	9.3	28.0	46.7
30	0.80	17.92	31.34	37.44	0.88	69.9	350.7	70.1	84.7	254.1	423.6
31	0.91	0.00	0.00	0.00	0.88	3.6	18.2	3.6	4.4	13.2	21.9
32	0.66	30.52	46.33	52.44	0.90	23.2	42.5	8.5	28.2	84.7	141.2
33	0.61	3.25	10.71	15.34	0.79	4.7	14.8	3.0	5.5	16.5	27.6
34	0.70	0.00	0.00	3.76	0.78	1.4	5.2	1.0	1.6	4.7	7.9
35	0.46	19.92	30.61	34.81	0.77	18.4	55.2	11.0	20.6	61.8	102.9
36	0.68	9.72	20.58	25.86	0.79	27.4	147.4	29.5	32.2	96.5	160.9
37	0.59	23.53	37.37	42.52	0.80	32.5	110.6	22.1	37.6	112.7	187.9
38	0.68	29.79	46.76	53.39	0.88	38.1	152.5	30.5	45.1	135.3	225.6
39	0.72	17.26	30.89	36.82	0.83	268.7	1381.3	276.3	326.5	979.4	1632.4
40	0.67	10.40	20.63	26.84	0.90	12.5	30.3	6.1	14.6	43.9	73.1

Table 2. Quick screening and estimation results for all evaluation reservoirs.

(continued)

Table 2. Continued

No.	t_D^0 (PV)	R_{D1} (%)	R_{D2} (%)	R_{D3} (%)	S_{CO_2} (PV)	Np ($\times 10^4$ t)	M_{CO_2t} ($\times 10^4$ t)	M_{CO_2e} ($\times 10^4$ t)	Min. stor. ($\times 10^4$ t)	Mid. stor. ($\times 10^4$ t)	Max. stor. ($\times 10^4$ t)
41	0.44	0.00	0.00	0.00	0.78	9.9	36.1	7.2	11.0	33.1	55.1
42	0.60	0.00	0.00	0.00	0.78	1.4	5.2	1.0	1.6	4.7	7.9
43	0.49	17.99	28.08	32.20	0.78	19.8	67.9	13.6	21.9	65.8	109.7
44	0.84	23.75	40.42	48.12	0.94	17.4	63.0	12.6	21.6	64.8	108.0
45	0.34	0.00	0.00	1.01	0.73	64.3	317.3	63.5	72.2	216.7	361.1
46	0.35	2.76	9.71	16.58	0.83	34.1	165.3	33.1	39.4	118.1	196.9
47	0.50	0.00	0.00	0.00	0.84	4.7	23.1	4.6	5.4	16.2	27.0
48	0.40	17.89	31.16	38.00	0.77	72.4	365.2	73.0	83.3	249.8	416.3
49	0.33	0.00	0.00	0.00	0.78	1.6	8.1	1.6	1.8	5.4	9.0
50	0.41	0.00	0.00	0.00	0.80	2.2	11.5	2.3	2.5	7.4	12.4
51	0.48	0.00	0.00	0.00	0.80	1.0	5.2	1.0	1.1	3.4	5.6
52	0.37	6.26	10.13	15.59	0.93	20.1	109.5	21.9	24.3	72.9	121.5
53	0.45	5.32	10.22	15.96	0.94	45.7	249.3	49.9	55.2	165.7	276.2
54	0.12	12.09	12.75	17.75	0.94	21.8	122.4	24.5	26.3	79.0	131.6
55	0.43	47.75	66.06	72.76	0.94	71.2	392.8	78.6	85.5	256.5	427.5
56	1.00	0.00	0.00	0.00	0.97						
57	0.85	0.00	0.00	0.00	0.96						
58	1.00	0.00	0.00	0.00	0.96						
59	0.87	19.50	34.65	42.40	0.96						
60	0.96	0.00	0.00	0.00	0.96						
61	1.00	6.94	19.07	27.29	0.99						
62	0.89	4.67	14.96	22.69	0.99	3.8	23.4	4.7	4.6	13.8	23.1
63	0.97	0.00	0.00	0.00	0.99	1.5	9.2	1.8	1.8	5.4	9.0
64	1.06	0.00	0.00	0.00	0.99						
65	0.93	0.00	0.00	0.00	0.95	0.3	1.7	0.3	0.3	1.0	1.7
66	0.92	0.00	2.15	9.02	0.95	1.5	9.3	1.9	1.8	5.4	9.0
67	0.87	0.00	7.92	15.19	0.97	5.5	34.0	6.8	6.5	19.6	32.6
68	0.89	2.78	12.58	19.71	0.95	0.3	1.8	0.4	0.3	1.0	1.7
69	0.89	0.00	0.00	0.00	0.96						
70	0.93	27.10	44.37	52.44	1.00	3.0	19.5	3.9	3.7	11.1	18.6
71	0.91	9.34	20.40	27.33	0.97	9.5	61.6	12.3	11.1	33.4	55.7
72	0.81	19.57	34.61	41.61	0.90						

Note: the blank cells represent reservoirs with very thin layers or a new field with a short production time and low primary recovery factor.

~43.1% in each field. The R_{D2} value varies between approximately 12.7% and 62.2%, and the maximum is 24.7~71.8%; the R_{D3} value varies between approximately 14.2% and 68.3%, and the maximum is 26.8~77.7%. The average value trends of R_D, as shown in Fig. 7, indicates that

the LF13-2, LF22-1, HZ26-1, HZ32-5, HZ32-2 and HZ26-1 oilfields have relatively higher R_D values, which suggests these oilfields have greater potential CO_2 EOR than those of other fields.

Dimensionless CO_2 storage is the only parameter for screening CO_2 storage potential. The statistical analysis results indicate that the S_{CO2} of 59 reservoirs (accounting for 82%) varies from 0.7P V to 1.0 PV, as shown in Fig. 8(a–b). The maximum S_{CO2} is 1.0 PV. The S_{CO2} of 27 reservoirs is less than 0.8 PV, 45 reservoirs have a S_{CO2} larger than 0.8 PV, and 24 reservoirs have a S_{CO2} that varies from 0.9 PV to 1.0 PV, accounting for 34% of the reservoirs – these reservoirs have the highest CO_2 storage potential, with S_{CO2} greater than 0.9 PV.

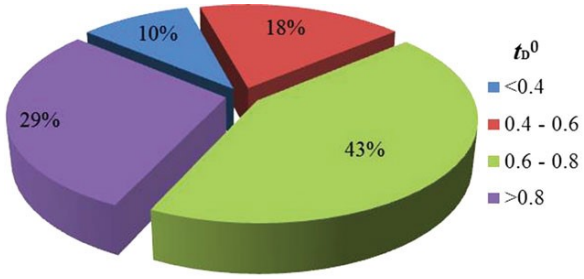

Figure 3. Pie graph of frequency percentages for dimensionless breakthrough time (t_D^0) for the reservoirs studied.

Table 3. Average and maximum analysis valuesof three RD values for the oilfields.

Oilfields	R_{D1} (Av.)	R_{D1} (Max)	R_{D2} (Av)	R_{D2} (Max)	R_{D3} (Av)	R_{D3} (Max)
HZ21-1	20.6	33.3	31.8	48.3	35.4	52.3
HZ26-1	23.8	32.5	37.3	49.5	42.1	55.6
HZ32-2	21.7	37.4	33.1	54.8	36.9	60.3
HZ32-3	16.2	30.2	24.9	47.3	28.3	54.0
HZ32-5	22.7	33.6	35.5	51.1	40.8	58.7
LF13-1	19.7	23.6	31.4	36.7	34.9	40.4
LF13-2	43.1	43.1	62.2	62.2	68.3	68.3
LF22-1	26.7	26.7	40.2	40.2	43.6	43.6
XJ24-1	7.7	29.4	14.2	46.8	18.0	54.6
XJ24-3	18.5	53.2	24.3	71.8	26.7	77.7
XJ30-2	8.3	16.5	12.7	24.7	14.2	26.8

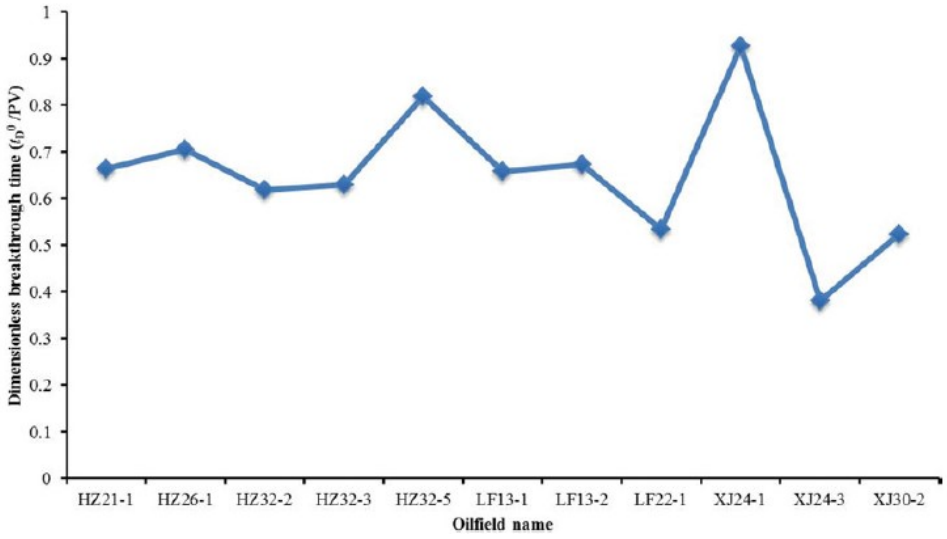

Figure 4. Average dimensionless breakthrough times for the oilfields.

Case study

Generally, an oilfield includes several layers with similar geological characteristics, therefore, it is important to screen these reservoirs quickly to identify the most economically attractive one for CO_2 flooding and storage. A case study of the HZ21-1 oilfield, which includes seven oil reservoirs, was discussed in this section (Fig. 7). The results show that M10 and L60 have the highest EOR recovery, with final (when 1.2 PV of CO_2 was injected) recoveries of >51% of the initial residual oil (at the start of CO_2 flooding). The L40Up reservoir has the second-highest recovery, and >40% of the initial residual oil was recovered by CO_2 flooding; t_D^0 is shorter in reservoirs L40Up, M10, L60, and L40low. In particular, in L40Up, oil recovery occurs at 0.61 PV CO_2 injection. The S_{CO2} values are approximately the same – 0.8 PV, in all reservoirs. This could be associated with the same pressure conditions being present because the amount of CO_2 stored is mainly affected by pressure in the reservoir, as shown in the S_{CO2} model equation.

According to the analyses above, M10 and L60 are the most promising reservoirs, followed by L40Up. Considering that the oil reserves of these three reservoirs are 70% of the total oil reservoirs over the HZ21-1 field, CO_2 EOR should be implemented in all three reservoirs to obtain the best flooding effectiveness. The reserves in the M10 reservoir are 33% of the total reserves and 2.7 and 1.7 times that in L60 and L40Up, respectively, so M10 would have the highest EOR potential among the six reservoirs.

Moreover, as the dimensionless recovery factor is predominantly determined by reservoir thickness; the thicker (such as M10) the reservoir, the more oil is recovered, which could be related to the stable gravity flooding style assumed in the quick screening model. t_D^0 mainly depends on S_{oi}; for example, L40Up has a higher residual oil before CO_2 flooding, so it recovers oil earlier.

Sensitivity analysis

Several input groups, including L, P_{inj}, P_p, S_{oi}, S_{owr}, and P_{MM}, affect the results of the screening model. Among these parameters, L, P_{inj}, and P_p are the engineering, which are adjustable, and S_{oi} and P_{MM} are the reservoir properties that are measured or calculated indirectly. The variance of these parameters will influence the final evaluation results, so a sensitivity analysis is needed to observe the influence degree of the inputs to the outputs of R_D, t_D^0 and S_{CO2} . A sensitivity analysis was applied to the M10 reservoir of the HZ21-1 oilfield as a case study. The input parameters were evaluated at five values, set at a 25% interval, according to the basic values of M10, as shown in Table 4. The range is from 50% to 150% of the basic values. Considering practical engineering, the reasonable range of injection pressure (P_{inj}) should be between the original formation pressure and fracture pressure; thus, the interval value of P_{inj} was set to 11% of the difference between the basic value and the original formation pressure. The highest pressure is the formation fracture pressure, 44.76 MPa, which is 1.5 times the lowest pressure of 29.84 MPa (original formation pressure), which is used to limit the value changes of the outputs. The sensitivity analysis results are shown in Fig. 9. The R_{D3} values are negatively related to P_{MM} and L and positively to S_{oi}, P_{inj}

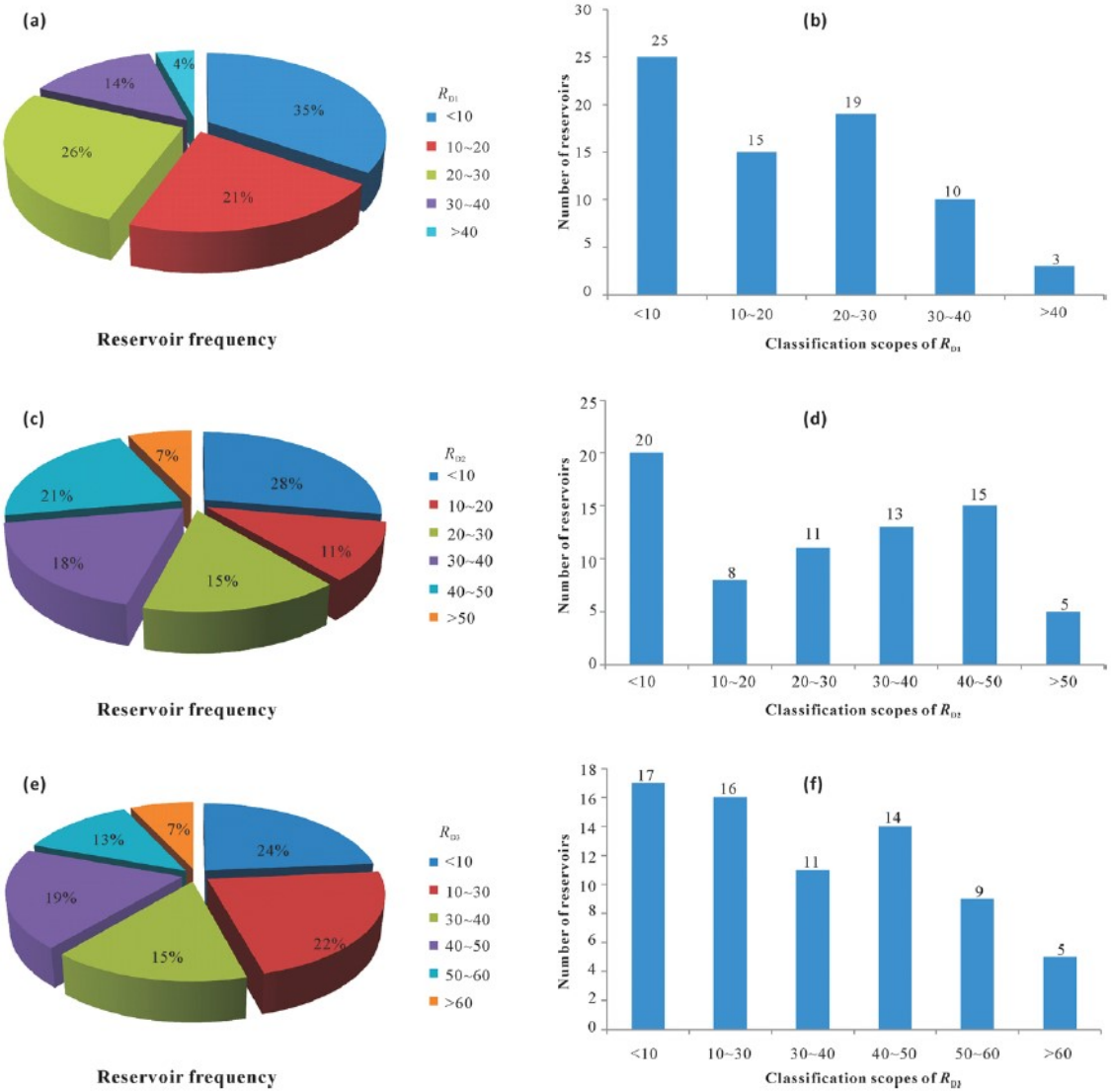

Figure 5. Pie graph of reservoir frequency percentage (left) and histogram of number of reservoirs (right) for three dimensionless recoveries, which show the frequencies and number in various scopes of dimensionless recovery classifications; a and b are for R_{D1}, c and d are for R_{D2}, and e and f are for R_{D3}.

and P_p, as shown in Fig. 9(a). With the exception of P_{MM}, the rest other input groups show a linear correlation with R_{D3}. According to the slope of the corresponding line segments in Fig. 9(a), the most important groups for R_D are S_{oi} and P_{inj}, and the change in R_D could be up to 45%. If the value of S_{oi} is greater than 30% or P_{inj} is larger than 44 MPa, R_{D3} is likely to exceed 60%. The production pressure (P_p) group can affect the recovery factor by 14%. The well distance (L) group is the least sensitive to R_D, which changes less than 10%. Figure 9(b) shows the sensitivity results of the dimensionless breakthrough time (t_D^0). t_D^0 is positively correlated with the injection pressure (P_{inj}) and negatively correlated with the other parameters including S_{oi}, P_{MM} and P_p. P_{MM} and P_{inj} are the most sensitive to t_D^0, followed by S_{oi}. The t_D^0 value could be up to 0.4 PV when S_{oi} changes from −50% to +50%. P_p has the lowest sensitivity to t_D^0, which only varies by 0.1 PV. In modeling S_{CO2} , only the pressure groups including P_{MM}, P_{inj} and P_p affect the density of CO_2 and amount of CO_2 stored. S_{CO2} is positively correlated to P_{inj} and negatively correlated to P_p and P_{MM}, as shown in Fig. 9(c). P_{inj} is the most sensitive to S_{CO2} , followed by P_{MM}, and P_p is the least sensitive. Although P_{inj} has the highest sensitivity on both

t_D^0 and S_{CO2}, the degree of sensitivity is different. When P_{inj} increases 0.2 times, t_D^0 would increase to 0.13 PV, and S_{CO2} would increase to 0.2 PV. The P_p influence is similar to that of P_{inj}, indicating that the sensitivity of S_{CO2} to the pressure is higher than that of t_D^0. When P_{inj} is > 41 MPa or P_{MM} < 16 MPa, S_{CO2} can become greater than 1.0 PV. The resultant sensitivity analysis diagrams show that the P_{MM} parameter is the only parameter that is negatively correlated with the result, and that has a concave curve type. If P_{MM} changes less than the basic value, the impact on R_D and t_D^0 are the greatest, when the P_{MM} value increases gradually, the influence on the evaluation output groups would reduce gradually. In brief, the high S_{oi} before CO_2 injection and low P_{MM} are beneficial to enhance the recovery factor and reduce the breakthrough time. A high injection pressure of CO_2 (P_{inj}) is advantageous to oil recovery (R_D) but delays the breakthrough time (t_D^0). The evaluated ranges in production pressure (P_p) andwell distance (L) have less of an effect on the recovery and breakthrough time. Obtaining higher oil production therefore relies mainly on the increase in injection pressure.

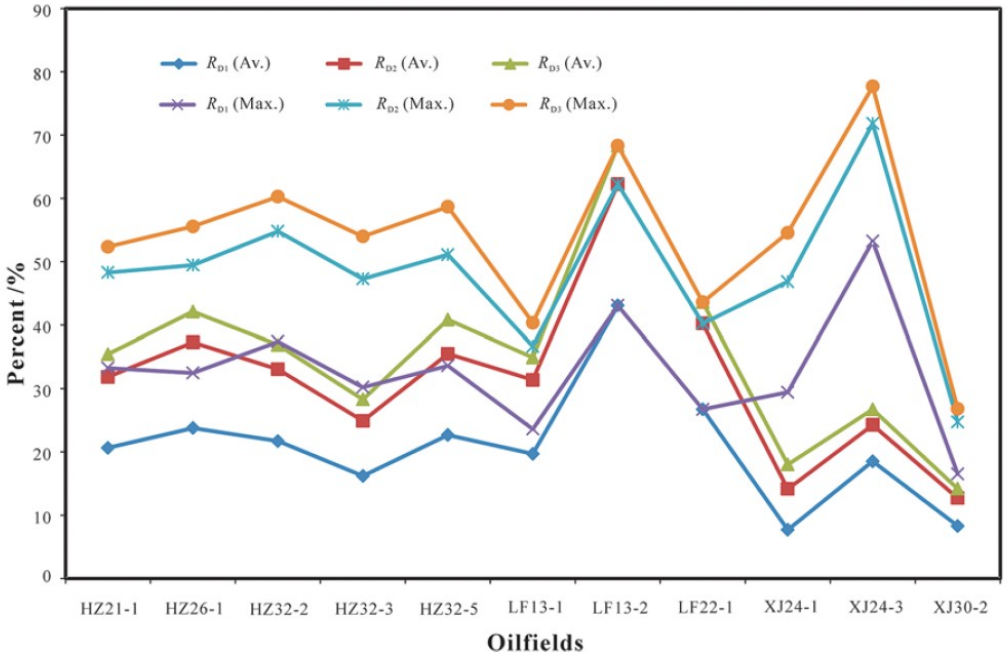

Figure 6. Correlation curves of the average and maximum values of three dimensionless recoveries for 11 oilfields.

CO_2 storage capacity

According to the results in Table 2 and Table 5, the theoretical storage capacity of the individual reservoirs varies from 1.4×10^4 t to 1178×10^4 t of CO_2, and at the oilfield level, it varies from 198×10^4 to 1923×10^4 t of CO_2. If a value of 0.25 is taken as the effective storage coefficient affected by all factors, the effective storage capacity ranges from 0.3×10^4 t to 294×10^4 t of CO_2 at reservoir level and 49×10^4 t to 481×10^4 t of CO_2 at the oilfield level. The total effective storage capacity for all reservoirs is 2269×10^4 t of CO_2, and it is 2633×10^4 t of CO_2 at the oilfield scale. According to the analogy method of Eqn (3), the storage capacity for the minimum, middle and maximum grades varies from 0.3~326.5×10^4 t of CO_2, 1.0 ~979.4×10^4 t of CO_2 and 1.7~1632.4×10^4 t of CO_2, respectively, at the reservoir scale and 73~710×10^4 t of CO_2, 218~2129×10^4 t of CO_2 and 363~3549×10^4 t of CO_2, respectively, at the oilfield scale. The total minimum grade capacity for all the reservoirs is 2936×10^4 t of CO_2,

and it is 3617×10^4 t of CO_2 for all the oilfields. The CO_2 storage capacity at the reservoir scale is approximately equal to that at the oilfield scale. The capacity for the middle grade from the analogy method is approximately equal to the theoretical storage capacity obtained in the above calculation of Eqn (1), and the effective storage capacity is approximately equal to the minimum grade capacity.

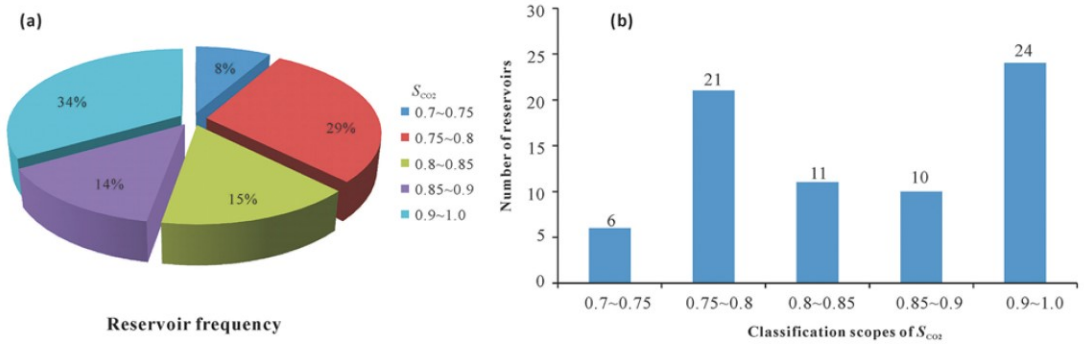

Figure 7. Results of EOR and CO_2 storage potential for seven oil reservoirs in the HZ21-1 field (Q is the ratio of the proven reserve of a reservoir over the total reserves of the field).

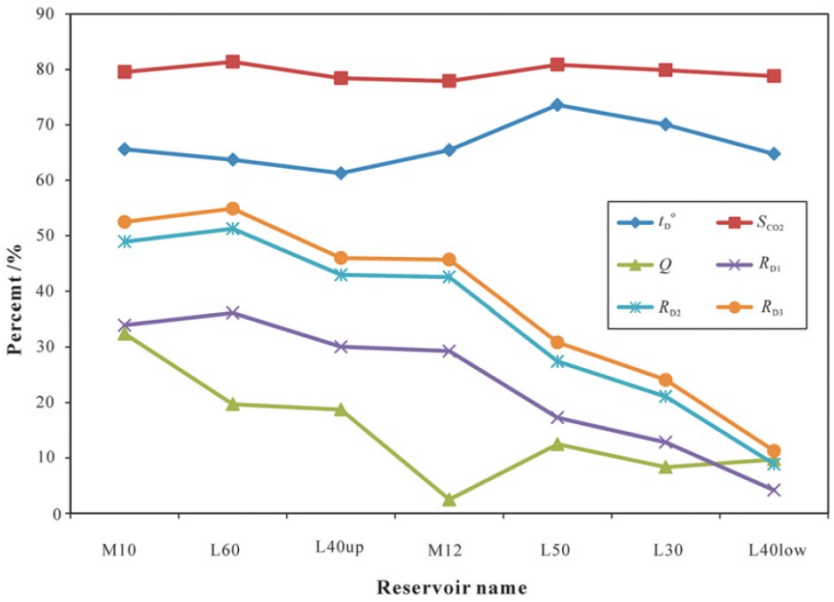

Figure 8. Pie graph of reservoir frequency percent (a) and histogram of number of reservoirs (b) for the dimensionless CO_2 storage (S_{CO2}, PV), which shows the frequencies and number of reservoirs in various scopes of the dimensionless recovery classifications.

Table 4. Parameters for the sensitivity analysis of the M10 reservoir.

L		S_{oi}		P_{inj}		P_p		P_{MM}	
(m)	L/base	(%)	S_{oi}/base	(MPa)	P_{inj}/base	(MPa)	P_p/base	(MPa)	P_{MM}/base
200	0.50	12.6	0.50	29.84	0.89	7.46	0.50	11.57	0.50
300	0.75	18.9	0.75	33.57	1.00	11.19	0.75	17.36	0.75
400	1.00	25.2	1.00	37.30	1.11	14.92	1.00	23.14	1.00
500	1.25	31.5	1.25	41.03	1.22	18.65	1.25	28.93	1.25
600	1.50	37.8	1.50	44.76	1.33	22.38	1.50	34.71	1.50

Table 5. Results of the calculation of the CO2 EOR potentials and CO2 storage capacities based on oilfield evaluation.

Oilfield name	*OOIP* (×10⁴ t)	R_f (%)	*Np* (×10⁴ t)	M_{CO_2t} (×10⁴ t)	M_{CO_2e} (×10⁴ t)	Min. Stor. (×10⁴ t)	Mid. Stor. (×10⁴ t)	Max. Stor. (×10⁴ t)	S_{CO_2} *PV* (av.)	R_{D3} % (av.)
XJ30-2	5638	51.00	634	1923	481	710	2129	3549	1.03	67.73
HZ26-1	4274	51.12	481	1408	352	572	1716	2860	1.03	64.69
HZ32-3	2967	62.90	334	1248	312	402	1206	2010	0.80	35.44
XJ24-3	3014	65.00	339	1387	347	397	1191	1985	0.84	42.10
LF13-1	1770	60.61	199	685	171	228	684	1141	0.80	36.90
XJ24-1	1646	56.55	185	780	195	224	672	1120	0.83	28.32
HZ21-1	1965	47.75	221	657	164	221	663	1105	0.93	40.83
LF22-1	1680	34.42	189	672	168	221	663	1104	0.75	34.91
HZ19-2	1129	33.43	127	460	115	156	468	780	0.91	68.32
HZ32-2	1088	44.90	122	362	90	143	428	713	0.72	43.60
HZ19-3	1030	27.76	116	411	103	138	413	689	0.97	18.02
HZ32-5	1051	50.26	118	343	86	134	401	669	0.85	26.74
LF13-2	1433	54.65	161	198	49	73	218	363	0.73	14.17

CO_2 EOR potential

According to Eqn (2), the additional produced oil reserves (N_p) due to CO_2 EOR varies from 1 to 392 × 10^4 t, and the total additional produced oil is 2510 × 10^4 t for all reservoirs. There are only five reservoirs with additional produced oil reserves greater than 100 × 10^4 t. At the oilfields scale, N_p varies from 116 to 634 × 10^4 t, and the total N_p is 3227 × 10^4 t. There are four oilfields with N_p potential greater than 300 × 10^4 t. The total additional potential due to CO_2 EOR at the reservoir scale is approximately equal to that at the oilfield scale. The critical value of the additional oil potential for the optimal CO_2 EOR site is 100 × 10^4 t for the individual reservoir and 300 × 10^4 t at the oilfield scale.

CO2 EOR and storage prospects

The objective of this study is to provide a quick way to identify CO_2 EOR and storage candidates in the PRMB and to provide quick screening and a preliminary reservoir-scale assessment of additional oil recovery and CO_2 sequestration capacity. The results of this assessment indicate that important oil recovery and CO_2 storage potential lies in the offshore oilfields through application and co-optimization of enhanced oil recovery and CO_2 storage. Both an increase in oil production and decrease in CO_2 (e.g., incidental storage) can be achieved by the implementation of CO_2 EOR projects. For these reasons, the CO_2 EOR and storage prospects in the oil reservoirs of the PRMB are promising.

The screening results indicate that the reservoir suitability for CO_2 EOR can be divided into five grades according to the reservoir characteristics as described by the dimensionless parameters and potential scales, as shown in Table 6. There are 13 reservoirs with the highest optimal grade, 16 reservoirs at the higher level and 18 reservoirs with a high grade for co-optimization of EOR and CO_2 sequestration; high ultimate recoveries (R_{D3}) and shorter breakthrough times (t_D) were predicted for all these scenarios. The third grade includes 18 reservoirs with high R_D, high S_{CO2}, and long t_D values, respectively. More than 40 oil reservoirs

are predicted to have a large potential with a high R_D (> 40%), S_{CO2} mostly between approximately 0.8~0.9 PV and t_D between 0.6 and 0.8 PV. These reservoirs mostly belong to seven oilfields, namely, the HZ26-1, HZ32-3, LF13-1, HZ21-1, HZ32-2, HZ32-5, and XJ24-3 oilfields.

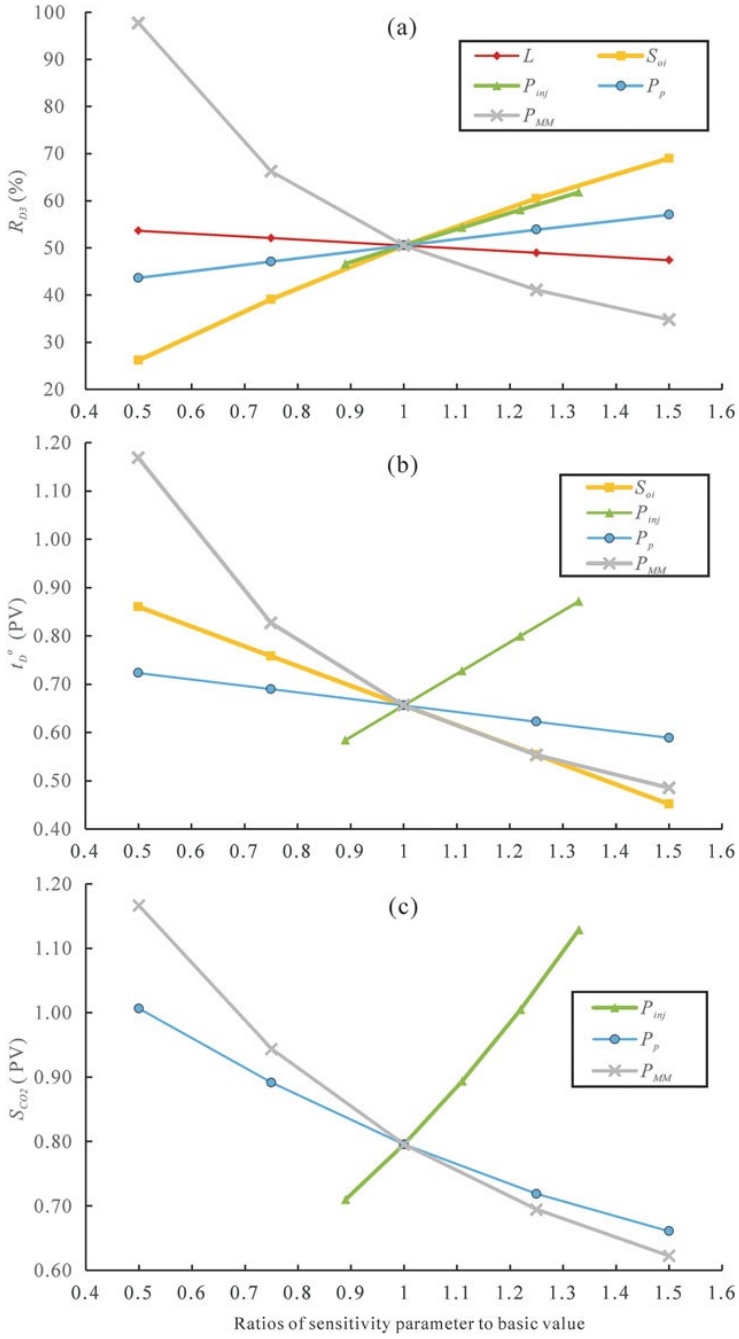

Figure 9. Results of sensitivity analysis regarding R_{D3} (a), t_D^0 (b) and S_{CO2} (c).

The reservoir characteristics of high porosity and high permeability and strong water-drive energy[17] indicate good connectivity and a stable formation pressure system, which is favorable for reservoir stability and reduces the risk from faulting and fracturing affected by CO_2 injection operations. The depressions in the PRMB have weaker seismic and fault activity, and only a handful of earthquakes with a magnitude (M) less than five are documented in the

historical records,[51,52] so these more stable characteristics provide favorable conditions for oil and gas accumulation and storage. More than approximately 100 wells were drilled for oil production in these oilfields.[17] It is believed that some of these wells are in poor condition or in need of repair after a long production time (>20 years). The potential risk of CO_2 leakage through wellbores would be a common problem in these fields, especially for the oilfields in an earlier development stage, because of the complex well conditions, including more sidetracking horizontal wells for offshore petroleum production. A more detailed study on the risk of CO_2 leakage along wellbores should therefore be carried out in these PRMB oil reservoirs.

Table 6. The suitability classification of reservoirs for optimal CO_2 EOR sites.

Type	Characters	Reservoir amounts	Suitability grade	Np ($\times 10^4$ t)	M_{CO_2e} ($\times 10^4$ t)
I	Highest R_D, high S_{CO_2}, and shortest t_D	13 reservoirs	Highest	433	370
II	Higher R_D, low S_{CO_2} and short t_D	16 reservoirs	Higher	731	1094
III	High R_D, high S_{CO_2}, and long t_D	18 reservoirs	High	601	480
IV	Low R_D, low S_{CO_2}, long t_D, thicker, lower OOIP	7 reservoirs	Low	477	484
V	Lower R_D, low S_{CO_2}, Long t_D, thickest and lowest OOIP	18 reservoirs	Lower	267	262

With respect to the economic factors, although the utilization efficiency of CO_2 and the existing infrastructure are the most critical factors, as the PRMB is still in the stage of active hydrocarbon exploration and production, it is important not to hinder the primary hydrocarbon development by EOR and CO_2 storage activities. The XJ oilfield cluster is still in an earlier stage of oil production and exploration. The LF and HZ oilfield clusters are in the first batch of oilfield development projects; after nearly 30 years of development, they have entered a high water-cut stage and required a new high-efficiency EOR technology. The application of CO_2 EOR in these oilfields should therefore be more economical for improved oil production and construction and operation costs of the offshore platform. Accordingly, the reservoirs from the LF and HZ oilfield clusters should be proposed for potential CO_2 EOR and storage candidate sites. Briefly, it can be concluded that the reservoirs in the LF and HZ oilfields are the most promising for CO_2 EOR and storage due to their large potential, structural stability, and the economic factors.

Discussion

Developing CO_2 EOR as a mechanism for creating opportunities for CO_2 storage has been shown to be possible with field experience from worldwide projects over more than 40 years. A challenging aspect is the lack of offshore CO_2 EOR experience, causing development of these opportunities to be slow. This paper represents an attempt to use a comprehensive 'quick look' and potential evaluation methodology to screen and assess offshore CO_2 EOR potential that can be proven by further data collection and more in-depth analysis. The multiparameter 'quick look' and calculation method allows us quickly to reduce the number of potential sites, to save time and allow more of the available resources to be used to optimize and evaluate the potential of the candidates. The process proposed in this paper sequentially and quantitatively considers (1) site optimization for CO_2 EOR, (2) the amount of CO_2 that can

potentially be stored, (3) the recovery growth potential, and (4) the additional oil potential at the reservoir scale. In fact, it is very difficult to determine these values quantitatively. Although using more reservoir property allows more in-depth screening and assessing, incomplete data and uncertain parameter values of both the reservoir properties and engineering parameters would be critical in influencing the accuracy of these results.

First, the limitations of the reservoir property parameters used in this method, including P_{MM}, S_{oi} and relative permeability (k), were generally estimated by simple calculation or experiential values, which are generally tested by experiments and simulations. Second, the engineering parameters, including injection well location, injection pressure, and well distance were set following the observed values. The sensitivity analysis shows that a reasonable injection pressure is important for CO_2 flooding and that the well spacing is not a very sensitive parameter; this information is important for offshore settings because of the high costs of wells and space limitations of offshore platforms. These engineering parameters therefore need to be further optimized through simulations and test analyses. Third, the critical output parameters, including M_{CO2e}, M_{CO2R}, N_p, t_D, S_{CO2} and R_D, which should actually be solved by numerical simulations, were simplified by using a polynomial fitting method in order to realize a quick evaluation and screening; the calculation and screening model therefore itself has some uncertainty. In addition, the base model of quick screening is based on the sandstone oilfields in Gulf of Mexico; although the oilfields of the PRMB are similarly marine sandstone oilfield, there are still some differences between both fields in terms of their reservoir properties and fluid properties, which can also create errors or uncertainties. The estimation of EOR potential and CO_2 storage capacity in each oil reservoir was calculated on the basis of reservoir properties such as original oil in place, recovery factor, and CO_2 utilization coefficient, whose values should be determined through numerical simulations and field tests.

Due to the limitations above, we would like to consider the methodologies proposed in this study as a preliminary attempt or test to screen candidate sites and quantify the potential of CO_2 EOR, and CO_2 storage in oil reservoirs of the PRMB. Ideally, this method indicates the suitability of CO_2 EOR and storage at the reservoir scale and calculates the additional oil production and CO_2 storage. The results can provide a basis for site screening for Guangdong offshore CCUS development. The most practical and matched EOR additional reserve, CO_2 utilization and storage capacity values should be determined through the application of various cutoffs, and reservoir simulations will be explored for potential sites in future work, case by case.

Conclusion

This paper represents an attempt to introduce methodologies for the quick assessment and screening of offshore CO_2 EOR potential and storage capacity at the reservoir scale. The quantitative approach can quickly reduce the numbers of potential EOR and sequestration sites, saving the time, and allowing more of the available resources to be used to evaluate the potential and optimize the candidates. The process proposed to use multiple (as many as possible) parameters of reservoir properties and engineering design to carry out dimensionless

screening and capacity evaluations for quick site assessment and optimization, which can allow for more in-depth screenings and assessments.

The results show that considerable oil recovery potential and CO_2 storage capacity lies in the offshore oilfields of Guangdong province through application of CO_2 EOR and storage in sandstone oilfields of the PRMB. The suitability of the reservoirs for CO_2 EOR can categorized into four grades, and more than 30 reservoirs in the upper two grades can be considered optimal candidate sites for CO2 EOR. The results also indicate that there is a potential for approximately 3227×10^4 t of additional oil production and 3617×10^4 t of CO2 storage capacity for all the oilfields. These large offshore resources will likely be exploited when a large amount of CO_2 has finally been captured and made available in onshore Guangdong province. The reservoirs such as HZ21-1, HZ32-3, LF13-1, and HZ26-1 from the LF and HZ oilfield clusters are the most promising candidate sites for CO2 EOR and storage projects.

The sensitivity analysis shows that high S_{oi} and low P_{MM} values are beneficial to CO_2 EOR. The injection pressure (P_{inj}) would have a more sensitive effect than production pressure (P_p) and well distance (L) on the CO_2 EOR and storage efficiency, so a proper higher injection pressure (P_{inj}) may enhance the potential of EOR while the initial oil and minimum miscible pressure are constant. Although the scale of the reserve for individual reservoirs or oilfields is relatively small, therefore, the considerable potential can improve by adjusting CO_2 EOR operations such as injection and production pressure managements.

There are several advantages to conducting offshore CO_2 EOR and storage projects in the Guangdong province offshore PRMB; these advantages include the availability of traps by demonstrated oil accumulations, abundance of exploration and development data, complete offshore development infrastructures, potentially plentiful CO_2 sources matched the oil reservoirs, and regional geological and structural stability. Furthermore, the combination of the drive to reduce CO_2 emissions due to Guangdong's low-carbon strategy and the selection of enhanced oil recovery technologies of high-water-cut oil production fields would make the PRMB a good location for CO_2 EOR projects.

Acknowledgements

We gratefully acknowledge funding by an open fund (PLC20180801) of State Key Laboratory of Oil and Gas Reservoir Geology and Exploitation (Chengdu University of Technology), the National Natural Science Foundation of China (No. 41372256), the PetroChina Innovation Foundation (No. 2015D-5006-0203), the Key Logic project of Department of Energy, USA (No. K600-797) and the Natural Science Foundation of Guangdong Province, China (No. 2015A030310372). The authors are also grateful for support from the UK-China (Guangdong) CCUS Centre and Gulf Coast Carbon Center of the Bureau of Economic Geology at The University of Texas at Austin.

References

[1] Dai Z, Zhang Y, Stauffer P, Xiao T, Zhang M, Ampomah W et al., Injectivity evaluation for offshore CO2 sequestration in marine sediments. Energy Procedia 114:2921–2932 (2017).

[2] Yang W, Peng B, Liu Q, Wang S, Dong Y and Lai Y, Evaluation of CO2 enhanced oil recovery and CO2 storage potential in oil reservoirs of Bohai Bay Basin, China. Int J Greenhouse Gas Control 65:86–98 (2017).

[3] Li L, Khorsandi S, Johns RT and Dilmore RM, CO2 enhanced oil recovery and storage using a gravity-enhanced process. Int J Greenhouse Gas Control 42:502–515 (2015).

[4] Karimaie H, Nazarian B, Aurdal T, Nøkleby PH and Hansen O, Simulation study of CO2 EOR and storage potential in a North Sea reservoir. Energy Procedia 114:7018–7032 (2017).

[5] Balch R, McPherson B and Grigg R, Overview of a large scale carbon capture, utilization, and storage demonstration project in an active oil field in Texas, USA. Energy Procedia 114:5874–5887 (2017).

[6] Li Q, Chen ZA, Zhang JT, Liu LC, Li XC and Jia L, Positioning and revision of CCUS technology development in China. Int J Greenhouse Gas Control 46:282–293 (2016).

[7] Pale Blue Dot Energy, Progressing development of the UK's strategic carbon dioxide storage resource: a summary of results from the strategic UK CO2 storage appraisal project, presented by Axis Well Technology and Costain team at the industry stakeholder event on 27th April and was formally released by ETI on 12th May, pp. 1–47 (2016).

[8] NETL, Preliminary evaluation of offshore transport and geological storage of Carbon Dioxide, Submitted by Southern States Energy Board and Interstate Oil and Gas Compact Commission Offshore Task Force, Norcross, Georgia, pp. 1–107 (2013).

[9] Compernolle T, Welkenhuysen K, Huisman K, Piessens K and Kort P, Off-shore enhanced oil recovery in the North Sea: The impact of price uncertainty on the investment decisions. Energy Policy 101:123–137 (2017).

[10] Zhou D, Li P, Liang X, Liu M and Wang L, A long-term strategic plan of offshore CO2 transport and storage in northern South China Sea for a low-carbon development in Guangdong province, China. Int J Greenhouse Gas Control 70:76–87 (2018).

[11] Kang P, Lim J and Huh C, Screening criteria and considerations of offshore enhanced oil recovery. Energies 9(1):44 (2016).

[12] Zhou D, Zhao D, Liu Q, Li X-C, Li J, Gibbons J, et al., The GDCCSR project promoting regional CCS-readiness in the Guangdong province, South China. Energy Procedia 37:7622–7632 (2013).

[13] GDCCSR-GIEC, Analysis of CO2 emission in Guangdong province, China, a summary report for project of feasibility study of CCS-readiness in Guangdong (GDCCSR) prepared by Guangdong CCS research team, Guangzhou, pp. 1–30 (2013).

[14] GDCCSR-SCSIO, Assessment of CO2 storage potential for Guangdong province, China, a summary report for project of feasibility study of CCS-readiness in Guangdong (GDCCSR) prepared by Guangdong CCS research team, Guangzhou, pp. 1–74 (2013).

[15] Li P, Zhou D, Zhang C, Zhang Y and Peng J, Potential of sub-seafloor CO2 geological storage in northern South China Sea and its importance for CCS development in south China. Energy Procedia 37:5191–5200 (2013).

[16] Li X, Zhou D, Li P, Wu Y, Liang X, Wei N, et al., CO2 offshore storage in China: research review and plan for demonstration project. Report No. D01/2015 released by UK-China (Guangdong) CCUS Centre, p. 46 (2015).

[17] Liu B, Development of Oil and Gas fields of China. Volume of oil and gas fields in eastern South China Sea. Petroleum Industry Press, Beijing (2011). (In Chinese.)

[18] Zhu W and Mi L, Atlas of Oil and Gas Basins, China Sea. Petroleum Industry Press, Beijing (2010). (In Chinese.)

[19] Zhu W, Mi L, Gao L and Gao Y, A review of China offshore hydrocarbon exploration in 2007. China Offshore Oil Gas 20(1):1–8 (2008) (in Chinese with English abstract).

[20] Huang Y, Guo H, Liao C and Zhao D, The study on prospect and early opportunities for carbon capture and storage in Guangdong province, China. Energy Procedia 37:3221–3232 (2013).

[21] Luo D, High Speed and Efficient Development Mode of Sandstone Oifields in Eastern Pearl River Mouth Basin, South China Sea. Petroleum Industry Press, Beijing (2013). (In Chinese.)

[22] Shaw J and Bachu S, Screening, evaluation, and ranking of oil reservoirs suitable for CO2-flood EOR and carbon dioxide sequestration. J Can Pet Technol 41(9):51–61 (2002).

[23] Núñez-López V, Holtz MH, Wood DJ, Ambrose WA and Hovorka SD, Quick-look assessments to identify optimal CO2-EOR storage sites. Environ Geol 54(8):1695–1706 (2007).

[24] Hendriks C, Graus W and Bergen F, Global Carbon Dioxide Storage Potential and Costs. Ecofys, Utrecht (2004).

[25] Rivas O, Embid S and Bolivar F, Ranking reservoirs for carbon dioxide flooding processes. SPE Adv Tech 2(1):95–103 (1994).

[26] Diaz D, Bassiouni Z, Kimbrell W and Wolcott J, Screening criteria for application of carbon dioxide miscible displacement in waterflooded reservoirs containing light oil. Society of Petroleum Engineers/DOE Improved Oil Recovery Symposium, Tulsa, OK (1996).

[27] Wood DJ, Lake LW, Johns RT and Nunez V, A screening model for CO2 flooding and storage in Gulf Coast reservoirs based on dimensionless groups. SPE Reservoir Eval Eng 11(3):513–520 (2008).

[28] Shook M, Li D and Lake LW, Scaling immiscible flow through permeable media by inspectional analysis. In Situ 16(2):311–349 (1992).

[29] Wood DJ, Creating a Quick Screening Model for CO2 Flooding and Storage in Gulf Coast Reservoirs using Dimensionless Groups. Bureau of Economic Geology, The University of Texas at Austin, TX (2006).

[30] Ramírez A, Hagedoorn S, Kramers L, Wildenborg T and Hendriks C, Screening CO2 storage options in The Netherlands. Int J Greenhouse Gas Control 4(2):367–380 (2010).

[31] Bachu S, Bonijoly D, Bradshaw J, Burruss R, Holloway S, Christensen NP et al., CO2 storage capacity estimation: Methodology and gaps. Int J Greenhouse Gas Control 1(4):430–443 (2007).

[32] Bachu S and Shaw JC, CO2 storage in oil and gas reservoirs in western Canada: Effect of aquifers, potential for CO2-flood enhanced oil recovery and practical capacity. In Greenhouse Gas Control Technologies 7, ed. by Rubin ES and Keith DW and Gilboy CF, Wilson M, Morris T, Gale J et al. Elsevier Science Ltd, Oxford, pp. 361–369 (2005).

[33] CSLF, Comparison between methodologies recommended for estimation of CO2 storage capacity in geological media by the CSLF task force on CO2 storage capacity estimation and the USDOE capacity and fairways subgroup of the regional carbon sequestration partnership program (phase 3), in Carbon Sequestration Leadership Forum, ed. by Bachu S, pp. 21–22 (2008).

[34] Bachu S, Bonijoly D, Bradshaw J, Burruss R, Christensen NP, Holloway S, Mathiassen O-M, Forum CSL, Phase II final report from the task force for review and identification of standards for CO2 storage

capacity estimation, estimation of CO2 storage capacity in geological media - phase 2 -. Carbon sequestration leadership forum Melbourne, Australia, p. 24 (2007).

[35] Goodman A, Hakala A, Bromhal G, Deel D, Rodosta T, Frailey S, et al., U.S. DOE methodology for the development of geologic storage potential for carbon dioxide at the national and regional scale. Int J Greenhouse Gas Control 5(4):952–965 (2011).

[36] Oldenburg CM, Screening and ranking framework for geologic CO2 storage site selection on the basis of health, safety, and environmental risk. Environ Geol 54(8):1687–1694 (2008).

[37] Li Q, Liu G, Liu X and Li X, Application of a health, safety, and environmental screening and ranking framework to the Shenhua CCS project. Int J Greenhouse Gas Control 17:504–514 (2013).

[38] Mathias SA, Hardisty PE, Trudell MR and Zimmerman RW, Screening and selection of sites for CO2 sequestration based on pressure buildup. Int J Greenhouse Gas Control 3(5):577–585 (2009).

[39] Oldenburg CM, Bryant SL and Nicot J-P, Certification framework based on effective trapping for geologic carbon sequestration. Int J Greenhouse Gas Control 3(4):444–457 (2009).

[40] Stevens SH, Kuuskraa V and Gale J, Sequestration of CO2 in depleted oil and gas fields: global capacity, costs and barriers. Proceedings of the Fifth International Conference on Greenhouse Gas Control Technologies (GHGT-5), ed. By Williams DJ, Durie RA, McMullan P, Paulson CAJ and Smith AY. CSIRO Publishing, Collingwood, VIC, Australia, pp. 278–283 (2001).

[41] Bachu S and Shaw JC, CO2 storage in oil and gas reservoirs in western Canada: effect of aquifers, potential for CO2-flood enhanced oul recovery and practical capacity. Greenhouse Gas Control Technol 1:361–369 (2005).

[42] Stevens SH, Sequestration of CO2 in Depleted Oil and Gas Fields: Barriers to Overcome in Implementation of CO2 Capture and Storage (Disused Oil and Gas Fields). Report for the IEA Greenhouse Gas R&D Programme (PH3/22), ed. by Stevens SH, Kuuskraa VA and Taber JJ. IEA, USA (1999).

[43] Shen P, Liao X and Liu Q, Methodology for estimation of CO2 storage capacity in reservoirs. Petroleum Explor Dev 36(2):216–220 (2009).

[44] Luo D, Yan Z, Liang W, Liu W and Gu K, The Practice and Understanding of Marine Sandstone Oil Field High Speed Development in Pear River Mouth Basin, South China Sea. Petroleum Industry Press, Beijing (2013). (In Chinese.)

[45] CNOOC EB, Memoir on the Development of China Hydrocarbon Fields, Vol. 27: The District of Eastern South China Sea. Petroleum Industry Press, Beijing (2011).

[46] Jarrell PM, Fox CE, Stein HS and Webb SL, Practical Aspect of CO2 Flooding. In: SPE Monograph Series, Society of Petroleum Engineers, Richardson, Texas, 22(4):15 (2002).

[47] Holm LW and Josendal VA, Effect of oil composition on miscible-type displacement by carbon dioxide. Soc Pet Eng J 22(1):87–98 (1982).

[48] Mungan N, Carbon dioxide flooding – fundamentals. J Can Pet Technol 20(1):87–92 (1981). 49. Mungan N, Carbon dioxide flooding as an enhanced oil recovery process. J Can Pet Technol 31(9):13–15 (1992).

[50] He L, Shen P, Liao X, Gao Q, Wang C and Li F, Study on CO2 EOR and its geological sequestration potential in oil field around Yulin city. J Pet Sci Eng 134:199–204 (2015).

[51] Zhong J, Active faults and seismic activities in Pearl River Mouth Basin and neighboring region. Tropic Oceanology 8(3):11–19 (1989).

[52] Ding Y, The active faults and seismic activity in the Pearl River Mouth Basin and its vicinity areas. Earthquake Res China 10(4):307–319 (1994).